Controlling the Electrografting of Polymers onto Transition Metal Surfaces through Solvent vs Monomer Adsorption

X. Crispin,[†] R. Lazzaroni,[†] V. Geskin,[†] N. Baute,[‡] P. Dubois,[‡,§] R. Jérôme,[‡] and J. L. Brédas*,[†]

Contribution from the Service de Chimie des Matériaux Nouveaux, Centre de Recherche en Electronique et Photonique Moléculaires, Université de Mons-Hainaut, Place du Parc 20, B-7000 Mons, Belgium, and the Centre d'Etude et de Recherche sur les Macromolécules (CERM), Université de Liège, Sart Tilman B6, B-4000 Liège, Belgium

Received May 18, 1998

Abstract: Electropolymerization of methacrylic monomers opens the possibility of chemically grafting a wide range of polymers onto transition metal surfaces. In this work, the electropolymerization of polyacrylonitrile and polyethyl acrylate is studied in different solvents; we experimentally confirm that the choice of solvent is a critical parameter for obtaining electrografted polymers. A density-functional theory−based study modeling the interaction of solvent (acetonitrile, dimethylformamide, and pyridine) or monomer (acrylonitrile and ethyl acrylate) molecules with the Ni(100) metal surface provides the means to classify the organic molecules with respect to their ability to interact with the surface. The surface binding-energy difference between monomer and solvent is introduced in a Frumkin-type isotherm. This allows us to rationalize the experimental observations in terms of a competitive adsorption at the metal surface between the monomer and the solvent. The first step in the electrografting mechanism thus appears to be the chemisorption of the monomer at the electrode surface before cathodic polarization is applied; the chemisorbed monomer is therefore the first species reduced, giving rise to an adsorbed reactive intermediate, which is thus able to start the polymerization of a grafted chain.

1. Introduction

Metal-coating by polymer films is of great interest for applications such as corrosion protection or surface functionalization. A major aspect of the coating is the stability of the polymer/metal interface.[1] A few years ago, a promising approach was proposed by Lécayon et al.,[2] who chemically grafted polyacrylonitrile (PAN) films onto metal surfaces via electropolymerization in the cathodic regime. This method produces a very stable polymer/metal interface; even when washed with a solvent of the polymer, the deposited film remains adherent to the metal surface.[3] The strong adhesion has been explained by the formation of metal−carbon chemical bonds.[4−7] Up to now, this method has been mainly restricted to two polymers: PAN and polymethacrylonitrile (PMAN).

The complexity of the electrografting mechanism and that of the experimental system (the nature of the monomer, solvent, electrode, and electrolyte salt all appear to be important) spurred numerous experimental works[2−4,6,8−12] as well as theoretical studies.[5,7,13−16] In particular, the experimental data have shown the importance of the chemical nature of the metal surface. On one hand, ellipsometric studies show that the reduction of the oxide initially present at the surface appears to be a prerequisite for PAN film deposition.[17] On the other hand, highly uniform and adherent thin films of PAN or PMAN can be deposited in a cathodic process on a series of metals (Ni, Cu, Fe, Pt); on others (Al, Zn), however, the polymer film appears to easily peel off.[2,8,13,18a]

In a more general context, a number of experimental studies have dealt with the adsorption of acrylonitrile (CH_2═CH−C≡N;

[†] Université de Mons-Hainaut.
[‡] Université de Liège.
[§] Present address: Service des Matériaux Polymères et Composites, Université de Mons-Hainaut.

(1) Lee, L. H. *Fundamentals of Adhesion*; Plenum Press: New York, 1991.
(2) Lécayon, G.; Bouizem, Y.; LeGressus, C.; Reynaud, C.; Boiziau, C.; Juret, C. *Chem. Phys. Lett.* **1982**, *91*, 506.
(3) (a) Tanguy, J.; Viel, P.; Deniau, G.; Lécayon, G. *Electrochim. Acta* **1993**, *38*, 1501. (b) Tanguy, J.; Deniau, G.; Augé, C.; Zalczer, G.; Lécayon, G. *J. Electroanal. Chem.* **1994**, *377*, 115. (c) Jérôme, R.; Mertens, M.; Martinot, L. *Adv. Mater.* **1995**, *7*, 807. (d) Mertens, M.; Calberg, C.; Martinot, L.; Jérôme, R. *Macromolecules* **1996**, *29*, 4910.
(4) Deniau, G.; Viel, P.; Lécayon, G.; Delhalle, J. *Surf. Interface Anal.* **1992**, *18*, 443.
(5) Bureau, C.; Defranceschi, M.; Delhalle, J.; Deniau, G.; Tanguy, J.; Lécayon, G. *Surf. Sci.* **1994**, *311*, 349.
(6) Jonnard, P.; Vergand, F.; Staub, P. F.; Bonnelle, C.; Deniau, G.; Bureau, C.; Lécayon, G. *Surf. Interface Anal.* **1996**, *24*, 339.
(7) Bureau, C.; Chong, D. P.; Lécayon, G.; Delhalle, J. *J. Electron Spectrosc. Relat. Phenom.* **1997**, *83*, 227.
(8) Boiziau, C.; Lécayon, G. *Surf. Interface Anal.* **1988**, *12*, 475.
(9) Tanguy, J.; Deniau, G.; Zalczer, G.; Lécayon, G. *J. Electroanal. Chem.* **1996**, *417*, 175.
(10) Bureau, C.; Deniau, G.; Viel, P.; Lécayon, G. *Macromolecules* **1997**, *30*, 333.
(11) Mertens, M.; Calberg, C.; Baute, N.; Jérôme, R.; Martinot, L. *J. Electroanal. Chem.* **1998**, *441*, 237.
(12) Baute, N.; Teyssié, P.; Martinot, L.; Mertens, M.; Dubois, P.; Jérôme, R. *Eur. J. Inorg. Chem.* **1998**, 1711.
(13) Fredriksson, C.; Lazzaroni, R.; Brédas, J. L.; Mertens, M.; Jérôme, R. *Chem. Phys. Lett.* **1996**, *258*, 356.
(14) Geskin, V.; Lazzaroni, R.; Mertens, M.; Jérome, R.; Brédas, J. L. *J. Chem. Phys.* **1996**, *105*, 3278.
(15) Bureau, C.; Deniau, G.; Viel, P.; Lécayon, G.; Delhalle, J. *J. Adhesion* **1996**, *58*, 101.
(16) Crispin, X.; Geskin, V.; Jérôme, R.; Lazzaroni, R.; Brédas, J. L. *Proceedings of the Second International Conference on Polymer-Solid Interfaces: From Model to Real Systems,* Pireaux, J. J. Delhalle, J. Rudolf, P., Ed.; Presses Universitaires de Namur: Namur, 1996; p 53−64.
(17) Bouizem, Y.; Chao, F.; Costa, M.; Tadjeddine, A.; Lécayon, G. *J. Electroanal. Chem.* **1984**, *172*, 101.

10.1021/ja981730y CCC: $18.00
Published on Web 12/22/1998

AN) from gas phase or liquid phase onto various metals: copper, gold, platinum, silver, and nickel.[19] For those metals, chemisorption takes place through the nitrile group of AN. Our theoretical work modeling the interaction between AN and metal surfaces indicates that AN chemisorbs on copper, nickel, and iron[14,16] by means of the nitrile group and the C═C double bond, whereas AN does not interact strongly with zinc.[13] The relation between the chemisorption of AN on Fe, Ni, Cu, and Pt surfaces and the electrografting of PAN films on these metal surfaces points out the importance of the adsorption of the monomer.

So far, one of the major drawbacks of the electrografting reaction has been the severe restriction on the choice of polymers that can be grafted. In this work, we show that the electrografting method used to obtain a strong metal/polymer interface can be extended to other vinylic monomers besides AN or methacrylonitrile (MAN), when the polymerization conditions chosen are adequate. The most substantial progress in that prospect comes from the possibility of polymerizing (meth)acrylic esters. Such a type of monomers can indeed bring several interesting functional groups into the polymer chain, enabling it to interact strongly with surrounding materials. Subsequent deprotection is expected to promote compatibility and even bonding of the grafted polymer with another phase (e.g., polymer matrix, biological medium), through groups such as hydroxyl or carboxylic acid. In this work, the interplay between the nature of the solvent and monomer is investigated for several solvent/monomer pairs to establish the criteria leading to polymer electrografting. We focus on the process of monomer adsorption at the electrode, which is the prerequisite for initiating the polymer grafting. The possibility that the adsorption of the monomer on to the surface can be hindered by solvent molecules chemisorbed on the metal surface is investigated. Adsorption at a metal surface from solution involves replacement of solvent molecules, either as individual molecules,[20,21] or as a solvent cluster,[22,23] by the new adsorbate from the bulk solution. The phenomenon of competitive adsorption between different species has already been observed in electrochemical experiments.[24] Note that a molecular description of the adsorption of organic compounds often used as solvent in electrochemistry is also of general interest for improving the description of the first layer of molecules at metal/solution interfaces.[25]

Here, we describe experimental results on the grafting (or absence of grafting) observed for a number of solvent/monomer pairs. The monomers used are AN and ethyl acrylate (CH_2═$CH-COOC_2H_5$; EA) and the solvents are acetonitrile ($CH_3-C\equiv N$; ACN), pyridine (C_5H_5N; PY), and *N*,*N*-dimethylformamide ($(CH_3)_2-N-CHO$; DMF). Next, we discuss molecular models representing the adsorption of these organic molecules on a nickel surface. From these model systems, we establish a classification between the solvent and monomer molecules in terms of adsorption energy. We then use the Frumkin adsorption model[24] to explain the experimental results qualitatively in terms of competitive solvent/monomer adsorption at the nickel electrode.

2. Experimental Section

All solvents and monomers were dried and distilled to get rid of residual water and other impurities. AN, EA, and ACN were dried over calcium hydride and distilled under reduced pressure. DMF was dried over phosphorus pentoxide and distilled at 70 °C under reduced pressure. PY was dried over potassium hydroxide for 2 h at 120 °C and distilled at 40 °C under reduced pressure. Tetraethylammonium perchlorate (TEAP) was heated in a vacuum at 80 °C for 12 h prior to use.

Voltammetry experiments were carried out with the selected monomer (from 10^{-2} to 2 M) dissolved in one of the three appropriate solvents containing TEAP as an electrolyte (5×10^{-2} M). The water content of these solutions, measured by the Karl Fischer method (Tacussel aqua processor), was ascertained to be <5 ppm. All the experiments were carried out in a glovebox at room temperature under an inert (<10 ppm in oxygen) dry atmosphere.

The apparatus used for the voltammetry experiments was a PAR-EG&G potentiostat (Model 273A). Electropolymerization of the monomers was achieved in a one-compartment cell (150 ml of solution), and the potentials were measured against a Pt pseudo-reference electrode. Two platinum foils (10 cm^2 each) were used as counter-electrodes. It has been shown previously that the solvent and the electrolyte are not electroactive in the range of potential used in these electropolymerization experiments.[18a] Also, the Pt pseudo-reference electrode is stable in the potential range considered here,[18b,18c] which means that the voltammograms are not affected by distortion from potential drift.

The nickel working electrodes, 2 cm^2 in area, were mechanically polished with an alumina suspension in water, washed with heptane and acetone, and finally annealed overnight in a vacuum at 180 °C. The surface oxide of the nickel electrode was reduced in a monomer-free solvent/TEAP solution in a first cell in the glovebox immediately before the electrode was transfered to another cell containing a monomer/solvent/TEAP solution. The transfer of the nickel electrode from one cell to the other within the glovebox ensures the absence of oxide at the metal surface.

After deposition of the polymer film on the metal electrode by electropolymerization, the electrode was carefully washed in a solvent of the deposited polymer. The polymer films were analyzed by IR spectroscopy with a BRUKER (Equinox IFS 66) FT-IR spectrometer equipped with a grazing angle accessory and a polarizer (Specac KRS-5).

3. Theoretical Approach

3.1. Molecular Models. Experimental data indicate that chemisorption of AN and probably of the other organic molecules used (see Section 4.2.2) occurs at the metal surface. Since chemisorption is a localized interaction, small models for the surface, typically clusters of nickel atoms, can be used. Such clusters can be accurately described by means of sophisticated quantum mechanical methods based on density-functional theory (DFT). A 16-atom cluster, $Ni_{16}(100)$, was chosen to model the nickel surface. This Ni(100) surface has a surface atomic density intermediate between that of the compact (111) surface and that of the open (110) surface; since the reactivity of the surface depends on the surface atomic density,[22] the Ni(100) can be considered as possessing an average reactivity of different faces of the polycrystalline nickel surface. Reconstruction of the Ni-(100) surface has been measured to be weak,[26] hence reconstruction is neglected in our modeling. The interatomic distances in $Ni_{16}(100)$ are fixed at the bulk interatomic distances (distance

(18) (a) Mertens, M. *Greffage de polymères sur des surfaces conductrices de l'électricité par électropolymérisation*; Ph.D. Thesis; Université de Liège, 1995. (b) Martinot, L.; Lopes, L.; Andrianne, B.; Gilet, F.; Lebon, F. *J. Radioanal. Nucl. Chem.* **1994**, *182*, 213. (c) Martinot, L.; Lopes, L. *Radiochim. Acta* **1996**, *75*, 105.

(19) (a) Loo, B. H.; Kato, T. *Surf. Sci.* **1993**, *284*, 167. (b) Gao, P.; Weaver, M. J. *J. Phys. Chem.* **1985**, *89*, 5040. (c) Parent, P.; Laffon, C.; Tourillon, G.; Cassuto, A. *J. Phys. Chem.* **1995**, *99*, 5058. (d) Xue, G.; Dong, J.; Zhang, J.; Sun, Y. *Polymer* **1994**, *35*, 723. (e) Perreau, J.; Reynaud, C.; Boiziau, C.; Lécayon, G.; Makram, C.; Gressus, C. L. *Surf. Sci.* **1985**, *162*, 776.

(20) Bockris, J. O. M.; Devanathan, M. A. V.; Müller, K. *Proc. R. Soc.* **1963**, *274A*, 55.

(21) Bockris, J. O. M.; Swinkels, D. A. J. *J. Electrochem. Soc.* **1964**, *111*, 736.

(22) Trasatti, S. *Electrochim. Acta* **1992**, *37*, 2137.

(23) Nikitas, P. *J. Electroanal. Chem.* **1994**, *375*, 319.

(24) (a) Gileadi, E. *Electrosorption*; Gileadi, E., Ed.; Plenum Press: New York, 1967; chap. 1. (b) Bockris, J. O.; Conway, B. E. *Modern Aspects of Electrochemistry*; Butterworth: London, 1964; Vol. 3, chap. 3 and 5.

(25) Parsons, R. *Electrochim. Acta* **1984**, *29*, 1563.

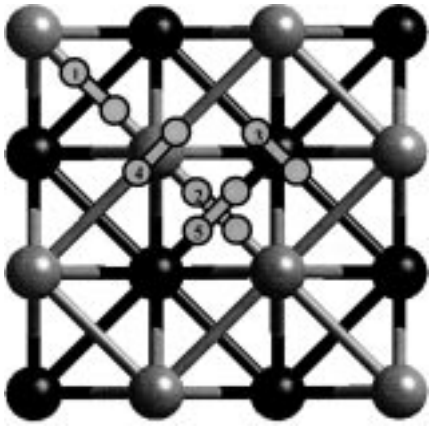

Figure 1. Illustration of the different positions taken by ethylene on the $Ni_{16}(100)$ cluster. The large black atoms are nickel atoms belonging to the bottom layer; those in gray are top-surface nickel atoms.

between nearest neighbors = 2.492 Å). The geometric structure of the $Ni_{16}(100)$ cluster is shown in Figure 1; the cluster is made of two layers, each containing 8 atoms.

The adsorption of solvent or monomer molecules onto the metal surface is modeled by a complex composed of the organic molecule interacting with the $Ni_{16}(100)$ cluster. The solvents are ACN, PY, and DMF; the monomers are AN and methyl acrylate (MA; $CH_2{=}CH{-}COOCH_3$). To keep the size of the organic molecule compatible with the surface area of the cluster, we take MA to represent the EA monomer used in the experiments. Replacing of the ethyl group by a methyl group is not expected to modify significantly the binding energy of the molecule with the surface, since that part of the molecule does not interact with the surface directly and the dipole moment of the whole species is not changed. The energy gain attributable to adsorption from solution also includes the energy of transfer from the bulk to the interface (linked to the solvent−solute interaction energy). The latter must be very similar for MA and EA, because of the absence of any specific interaction in their solutions and the similarity in the dipole moments and homomolecular interaction energies (as we judge from vaporization enthalpies) for both solutes. Therefore, we are confident that the adsorption behavior of MA and EA must be similar in gas phase as well as in solution.

After optimizing the geometry of the complex with the nickel cluster structure kept fixed, the binding energy is evaluated as the difference between the total energy of the complex and the sum of the total energies of the two isolated parts (the organic molecule and the nickel cluster). The aim of calculating these binding energies is not to determine adsorption energies accurately but to establish the relative ability of the molecules to interact with the nickel surface (obtaining absolute values of the chemisorption energy of a molecule on a metal surface from cluster calculations is well-known to be not straightforward[27]).

Competition between the adsorption of solvent and monomer is then evaluated by comparing the calculated binding energies. This comparison is only qualitative since several effects are not taken into account:[23] heterogeneity of the polycrystalline metal surface leading to different reactivities for different sites, lateral intermolecular interactions, solubility difference between that of the monomer and the solvent, influence of the electrolytic salt and electric field at the vicinity of the metal surface (which is expected to be weak when no external potential is applied to the electrode),[28] and entropic changes due to adsorption.[29] In Section 5, we discuss the validity of these approximations and then use the Frumkin isotherm [24] to explain qualitatively the experimental results on the basis of the theoretical results.

3.2. Methodology. The calculations were performed in the framework of the DFT method [30] (as implemented in the DMol program[31]). This first-principle method includes a significant part of the electron correlation energy, which is essential for a correct description of transition metal compounds. The chosen basis set is DNP (double-ζ numeric with polarization). The core orbitals are frozen during the self-consistent field (SCF) iterations and a medium mesh size is used for the calculations.[31] Geometry optimizations are carried out with the eigenvector-following algorithm by Baker,[32a] within the local spin density approximation (LSD), using the Vosko−Wilk−Nusair exchange-correlation potential.[33a] This algorithm was improved to optimize the geometry in Cartesian coordinates[32b] and to introduce constraints (fixed atoms) in Cartesian coordinates by use of an efficient Lagrange multiplier algorithm.[32c] The geometry optimizations are unconstrained except for the distances between metal atoms, which are kept at the bulk crystal values. The LSD approximation is well-known to provide reliable adsorption geometries of adsorbates but overestimates binding energy.[34]

On the basis of the LSD-optimized geometries, the binding energies are obtained by calculations that include, throughout the SCF iterations, both the gradient-corrected (GC) exchange potential by Becke[33b] and the gradient-corrected correlation potential by Perdew and Wang.[33c] For the calculations on the ethylene molecule adsorbed on the nickel cluster (see below), both the geometry optimization and the binding energy evaluation are performed at the GC level.

4. Results

4.1. Experimental Results. 4.1.1. Electrochemical Reduction of AN in ACN, DMF, and PY. AN is well-known to lead to grafting onto transition metals (e.g.; Ni, Cu, Fe, Pt) when electropolymerized in ACN,[2,3a,4,8] which is a nonsolvent for PAN. The formation of grafted PAN has also been observed in a good solvent of the polymer such as DMF.[3c,3d] In a recent paper, Mertens et al.[11] showed the possibility of grafting PAN in PY, another nonsolvent of the polymer. In all cases, the deposited films resist washing by a solvent of PAN (e.g., DMF). Grafted PAN is therefore obtained by direct polymerization of AN, whatever the solvent used (ACN, DMF, or PY), for the range of AN concentration investigated ($5 \times 10^{-2} - 2$ M]. Note that electrochemistry studies by Tanguy et al.[3a,3b,9] indicate that the electrografting reaction also takes place for MAN at high concentration on transition metal electrodes in ACN, which is a solvent of PMAN.

(26) Demuth, J. E.; Marcus, P. M.; Jepsen, D. W. *Phys. Rev. B* **1975**, *11*, 1460.
(27) (a) Panas, I.; Schüle, J.; Siegbahn, P.; Wahlgren, U. *Chem. Phys. Lett.* **1988**, *149*, 265. (b) Crispin, X.; Bureau, C.; Geskin, V.; Lazzaroni, R.; Brédas, J. L.
(28) Parsons, R. *J. Electroanal. Chem.* **1963**, *5*, 397.
(29) (a) Everett, D. H. *J. Phys. Chem.* **1981**, *85*, 3263. (b) Mulder, W. H. *J. Chem. Phys.* **1995**, *103*, 6164.
(30) Parr, R. G.; Yang, W. *Density-Functional Theory of Atoms and Molecules*; Oxford University Press: New York, 1989.
(31) (a) Delley, B. *J. Chem. Phys.* **1990**, *92*, 508. (b) Delley, B. *New J. Chem.* **1992**, *16*, 1103. (c) Ellis, D.; Painter, G. *Phys. Rev. B.* **1968**, *56*, 2887.
(32) (a) Baker, J. *J. Comput. Chem.* **1986**, *7*, 385. (b) Baker, J.; Hehre, W. J. *J. Comput. Chem.* **1991**, *12*, 606. (c) Baker, J. *J. Comput. Chem.* **1993**, *14*, 1085.
(33) (a) Vosko, H.; Wilk, L.; Nusair, M. *Can. J. Phys.* **1980**, *58*, 1200. (b) Becke, D. *Phys. Rev. A* **1988**, *38*, 3098. (c) Perdew, J. P.; Wang, Y. *Phys. Rev.* **1992**, *B45*, 13244.
(34) Ziegler, T. *Chem. Rev.* **1991**, *91*, 651.

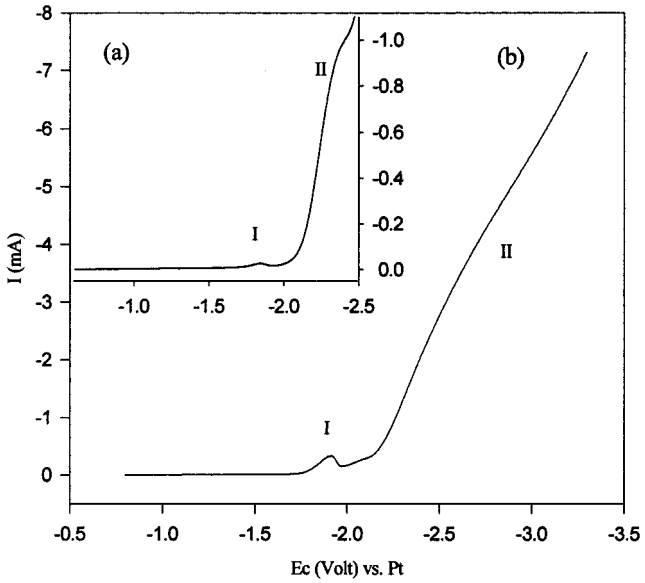

Figure 2. (a) Voltammetry of AN on nickel in a 0.05 M TEAP solution in DMF; [AN] = 0.5 M; $\nu = 20$ mV·s^{-1}. (b) Voltammetry of ethyl acrylate on nickel in a 0.05M TEAP solution in dimethylformamide; [EA] = 2 M; $\nu = 20$m V·s^{-1}.

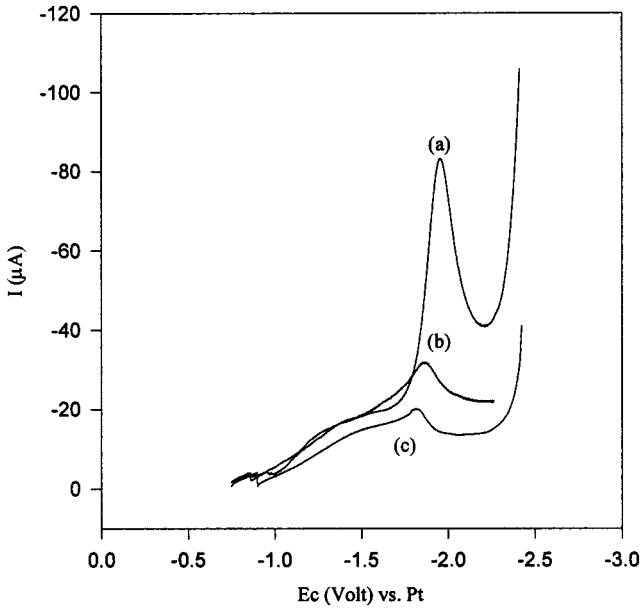

Figure 3. Voltammetry of AN on nickel in a 0.05M TEAP solution in pyridine: (a) [AN] = 2×10^{-2} M; (b) [AN] = 5×10^{-2} M; (c) [AN] = 0.1 M; $\nu = 20$ mV·s^{-1}.

Table 1. Intensity of the Current within Peak I for Various AN Concentrations in Acetonitrile, Pyridine, and Dimethylformamide; $\nu = 20$m V·s^{-1}

solvent	solvent for PAN	[AN] M			
		5×10^{-2}	0.1	0.5	2
ACN	no	*a*	370 μA	30 μA	25 μA
PY	no	25−30 μA	15−20 μA	*b*	*b*
DMF	yes	*a*	95 μA	20 μA	15 μA

[a] Peak I superimposed on peak II. [b] Peak I intensity too weak to be detected.

A typical voltammogram following the electrografting reaction is characterized by two peaks. The first one, often called "prepeak" (Figure 2a, peak I), does not appear in traditional electropolymerization reactions;[35] it is specific of the electrografting reaction. The major peak (Figure 2a, peak II) is called a "diffusion peak," since the current density linearly in this region varies with respect to the square root of the scan rate,[3b,3d] which is typical of diffusion-controlled electrochemical reactions. Peak II thus arises from tunnel charge transfer from the cathode to the monomer in solution. For AN, this charge transfer leads to the formation of radical anions in solution; those species are then believed to dimerize into dianions, which can initiate the anionic polymerization.[36]

Since the prepeak is specific to the electrografting reaction, various studies have focused on the features of this peak. Two hypotheses have been proposed to explain the growing mechanism of grafted PAN films in relation with the presence of this prepeak: anionic polymerization[2] or free radical polymerization.[3c] The current density related to the prepeak is Faradic; thus the presence of a prepeak is generally considered to reflect the fact that adsorption processes of electroactive species are involved in the electrochemical reaction.[37]

For AN electropolymerization in ACN and DMF, Mertens et al.[3d,11] found a shift toward less-cathodic potentials and an amplitude decrease for increasing monomer concentration. Figure 3 shows that such a typical concentration effect is also observed for AN polymerization in PY. Table 1 contains the current density of the prepeak recorded for increasing AN concentration in the three electrochemical media. These results suggest that the electrografting mechanism for AN is the same whatever the solvent used (ACN, DMF, PY). A similar concentration effect on the prepeak has been observed by Tanguy et al. for MAN in ACN.[3b]

The concentration effect on the reduction potential and amplitude of the prepeak appears to correspond to the electrochemical model by Wopschall and Shain[37] in which, after charge transfer, the product of reduction is adsorbed onto the cathode. This model is at the origin of the hypotheses that propose the prepeak is related to the adsorption of the product of an irreversible reduction during the electrografting mechanism of PMAN.[3b,9]

The microbalance measurements show a quartz frequency variation associated to the formation of PAN at the metal surface, which goes with the appearance of the prepeak.[11] A similar behavior is observed for PMAN.[9] It is thus clear that grafted polymer chains are formed at the prepeak. The formation of the polymer on the electrode surface is then expected to induce a blocking effect, hence the sharp decrease of the current.[3d,9] This would lead to the appearance of a maximum in the voltammetric curves, i.e., the prepeak. Direct electron transfer from the electrode to an AN monomer in solution would then require higher energy, which is consistent with the presence of the major peak at higher potentials relative to the initial electrochemical process.[3d] Mertens et al. explained the evolution of the prepeak with the monomer concentration in the following way: since the current density of the prepeak is inhibited by PAN film formation, then the larger the AN concentration, the faster the polymerization, and the quicker the current density drop.[3d] The resistance of the deposited PAN film to washing in a polymer solvent points out the highly stable interaction between the metal and a PAN film formed in the potential range of the prepeak, whatever the solvent used (ACN, DMF, PY).

Here, on the basis of new experimental and theoretical data presented in the following sections, we propose a new insight

(35) Funt, B. L.; Williams, F. D. *J. Polym. Sci. A* **1965**, *2*, 865.
(36) Bhadani, S. N.; Ansari, Q.; Gupta, S. K. S. *J. Appl. Polym. Sci.* **1992**, *44*, 121.
(37) (a) Wopschall, R. H.; Shain, I. *Anal. Chem.* **1967**, *39*, 1514. (b) Wopschall, R. H.; Shain, I. *Anal. Chem.* **1967**, *39*, 1535.

Table 2. Intensity of the Current (μA) within Peak I for Various Ethyl Acrylate Concentrations in DMF and PY; $\nu = 20$ mV·s^{-1}

	[EA] M			
	0.1	0.5	1	2
DMF	*a*	500	400	300
PY	*a*	600	300	350

[a] Peak I superimposed on peak II.

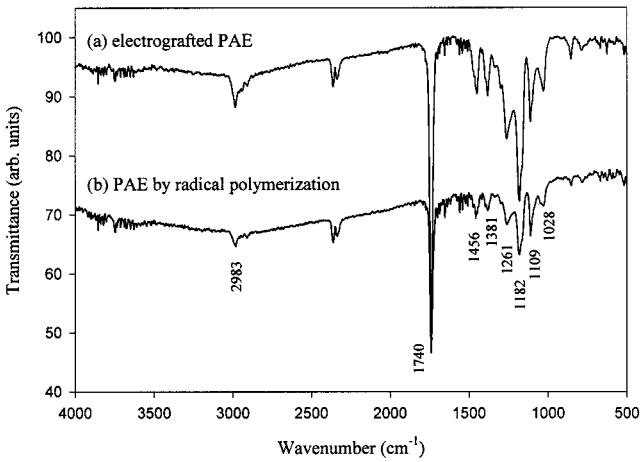

Figure 4. IR absorption spectra of (a) a PEA film deposited on nickel from a solution of [EA] = 2 M in DMF at the potential of peak I; (b) a PEA film synthesized by radical polymerization.

into the mechanism of formation of grafted polymer chains. Our results indicate that the first stage of the electrografting mechanism is the monomer adsorption onto the metal surface, and that the prepeak corresponds to the reduction of the previously adsorbed monomers rather than to the adsorption of the product of an irreversible reduction occurring in solution.

4.1.2. Electrochemical Reduction of EA in ACN, DMF, and PY. In this section, we describe a series of experimental results relative to a recently electrografted monomer: EA. Cathodic polarization has been carried out over an extended range of EA concentrations (5×10^{-2}−2 M) in ACN, but no grafted polymer film has been observed. Only one reduction peak of high intensity is observed in the voltammogram. This unique peak is undoubtedly related to a diffusion-controlled process, since its current increases and it shifts toward more-cathodic potentials when EA concentration is increased, at constant voltammetric scan speed. The electrochemical reaction is followed by polymerization in solution.

Similar experiments have been carried out in DMF. At EA concentration >0.5 M, a prepeak appears (Figure 2b) and a polyethyl acrylate (PEA) film is formed on the nickel surface despite the solubility of PEA in DMF, a clear indication that grafting of PEA has occurred. The separation between the two peaks increases and the current density of the prepeak decreases for a further increase in monomer concentration (Table 2). These observations are similar to those found for AN in various solvents, a situation for which a grafting is definitely established. IR absorption spectroscopic data (Figure 4a) confirm that the deposited film indeed consists of PEA, since its IR spectrum is identical to that obtained by radical polymerization (Figure 4b). The absorption band at 1740 cm^{-1} is characteristic of the carbonyl group and the band at 1182 cm^{-1} is related to C−O stretching. The C−H stretching modes of the polymer are represented by the absorption band at 2983 cm^{-1}. Note that the peaks observed around 2350 cm^{-1} are for residual carbon dioxide.

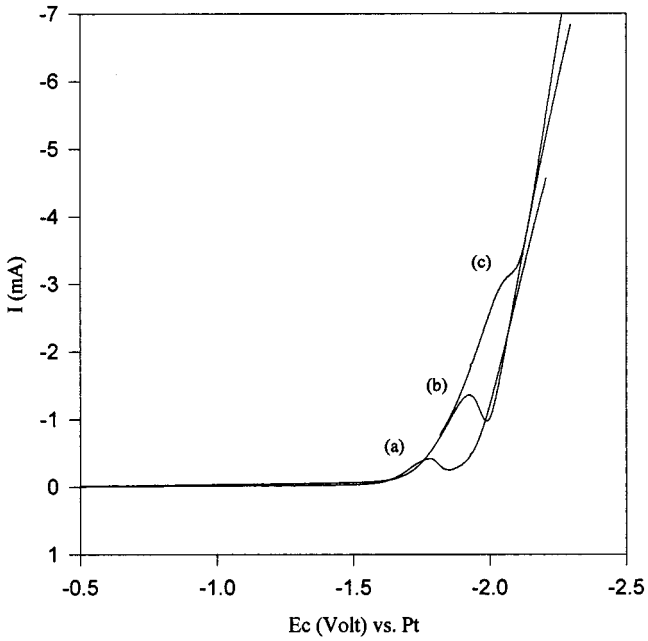

Figure 5. Voltammetry of EA (1 M) on nickel ($\nu = 20$ mV·s^{-1}) in DMF solution, illustrating the dependence of peak I current on the addition of ACN: (a) without ACN; (b) +3% ACN in volume; (c) +12% ACN in volume.

When PY is used as the solvent, at the lowest concentration of EA (10^{-2} M) shows only the diffusion peak, and no grafted polymer film is formed. For higher concentrations, there is no significant difference between the voltamperograms recorded in PY and DMF, (Table 2); the values of the current remain practically unchanged when PY is substituted for DMF, all the other conditions being the same. Hence, a grafted polymer film, identified as PEA by IR spectroscopy, is also produced in PY.

To estimate to what extent the electrografting signature of EA could be perturbed by the presence of ACN, we also investigated the reduction of EA in DMF added with ACN. Figure 5 compares the voltammetric cathodic scans of a 1 M ethyl acrylate solution in DMF modified by an increasing amount of ACN. The monomer concentration is kept unchanged in all the experiments. When EA is electrografted in DMF, the current of the prepeak is ~400 μA (Figure 5a). When the relative amount of ACN in the EA/DMF solution is increased, the current density of the prepeak increases, whereas the separation between the prepeak and the main peak decreases (Figures 5b, 5c). The dependence of the peak I current density on the ACN percentage in the EA/DMF solution is consistent with the fact that the EA concentration at the cathode is reduced because of the presence of ACN. This observation suggests that ACN competes with the monomer for adsorption onto the cathode. Further details on these experiments are the subject of another experimental work.[12]

4.2. Theoretical Results. 4.2.1. Evaluation of the Metal Cluster as a Model Surface for Adsorption: Ethylene on Ni(100). When using cluster−adsorbate complexes with relatively large adsorbates, as in this study, various aspects need to be stressed. In most cases, these adsorbates possess several chemical groups likely to interact with the metal surface. The number of possible positions on the surface is subsequently more than for an adsorbate that interacts with only one site (e.g., on-top CO). Then, there are different adsorption geometries corresponding to local minima of the Born−Oppenheimer potential surface. With the cluster used here to model the surface, some adsorption geometries, such as those involving

Table 3. Geometric Structure and Binding Energy of Ethylene Adsorbed at Different Positions on $Ni_{16}(100)$ (see Figure 1)

	C═C (Å)	C-Ni (Å)	C-Ni_{edge} (Å)	E_b (kcal/mol)
C_2H_4	1.333			
$C_2H_4^1$-$Ni_{16}(100)$	1.438	2.05	1.92	−27
$C_2H_4^2$-$Ni_{16}(100)$	1.462	2.04		−20
		2.04		
		different Ni atoms		
$C_2H_4^3$-$Ni_{16}(100)$	1.477	2.15	2.15	−21
		2.16	2.15	
		different Ni atoms	different Ni atoms	
$C_2H_4^4$−$Ni_{16}(100)$	1.420	2.07		−15
		2.07		
		both to the same Ni		
C_2H_4-Ni[a]	1.454	1.97		
		1.97		
		both to the same Ni		
$C_2H_4^5$-$Ni_{16}(100)$				no chemisorption

[a] From ref 38b.

edge atoms, may not be representative of adsorption on the infinite metal surface. To evaluate the capacity of our metal cluster to model the adsorption of molecules likely to be π-bonded, we have carried out a preliminary study of the surface reactivity of $Ni_{16}(100)$ versus ethylene. Ethylene is used for this test case because the numerous theoretical and experimental studies dealing with its adsorption on Ni(100).[38]

Five positions of ethylene on the $Ni_{16}(100)$ surface are considered (Figure 1). As a starting point for geometry optimization ethylene is located close to the surface (≅2 Å). After geometry optimization at the GC level, ethylene is found to be chemisorbed on the surface cluster. The geometric features of this chemisorption are summarized in Table 3. In the adsorption geometries labeled 1 and 2 in Figure 1, ethylene is bound to 2 metal atoms, with binding energies of −27 and −20 kcal/mol, respectively. On an infinite surface, these two locations would be equivalent; the higher binding energy found here for system 1 reflects the fact that one of the nickels this ethylene binds is an edge atom, which is less saturated. The adsorption geometry of ethylene in complex 2 involves two nickel atoms having the same number of nearest neighbors, as do actual surface atoms. Hence, this complex is probably a better model for the adsorption of ethylene on Ni(100). Ethylene is chemisorbed via four nickel atoms in adsorption geometry 3, which has a binding energy of −21 kcal/mol. Finally, adsorption configuration 4 involves only one nickel atom, for which the binding energy of ethylene is −15 kcal/mol. This complex, with ethylene bound to a single nickel atom, is similar to the simple [Ni−C_2H_4] complex theoretically studied with a correlated complete active space−SCF method (see Table 3).[38b] In position 5, no ethylene chemisorption occurs; in this position, the π molecular orbitals are probably not properly oriented to interact with the nickel surface.

At low temperature (130 K), near-edge X-ray absorption fine structure (NEXAFS)[38d] and high-resolution electron energy-loss spectroscopy (HREELS) experiments[38c] indicate that ethylene is chemisorbed flat on the Ni(100) surface by means of $2p_\pi$ atomic orbitals. From the NEXAFS data, the C═C bond length is evaluated to be 1.46 Å[38d]—exactly the same bond length calculated in the [C_2H_4−$Ni_{16}(100)$] complex 2, where ethylene interacts with two nickel atoms (Table 3). This confirms that complex 2 can be considered a good model for ethylene adsorption on Ni(100). The validity of this model is further confirmed by the LEED c(2 × 2) pattern obtained when ethylene is adsorbed on Ni(100) at low temperature;[38a] this pattern suggests a coverage of one ethylene molecule for two nickel atoms, that is, as in the [C_2H_4−$Ni_{16}(100)$] complex 2 of Figure 1.

The first part of this theoretical study indicates that the first four adsorption positions of ethylene have rather similar stabilities; this is in contrast to other adsorbates (e.g., H on W clusters[39]) where the binding energy changes dramatically (up to 60 kcal/mol) with respect to the adsorbate position on the cluster. This result thus points to a relatively flat Born−Oppenheimer potential surface for such an adsorbate in interaction with the $Ni_{16}(100)$ surface. No dramatic changes in binding energies are then expected when a larger adsorbate, that is, the monomer and solvent molecules considered in this work, is put at different positions on the surface, provided its π-moieties (nitrile, vinyl, carbonyl) interact via the first four positions described above. A complete geometry optimization of a large adsorbate interacting via several of its atoms with $Ni_{16}(100)$ is therefore expected to provide a good model for evaluating the binding energy of the adsorbate. We should then be able to classify the adsorbates according to their ability to interact with $Ni_{16}(100)$, a classification that could then be transferred to the actual Ni(100) surface.

4.2.2. Adsorption Geometries. 4.2.2.1. Acetonitrile on Ni-(100). ACN is commonly used as a solvent in electrochemistry and its chemisorption onto metal electrodes has been extensively studied.[40] Despite the chemisorption of ACN onto a metal electrode, the chemisorbed molecules can be displaced by other molecules coming from solution, as is the case for an ACN/dimethyl sulfoxide solution on a gold electrode.[40e] From ultrahigh vacuum studies, ACN is found to chemisorb on nickel.[41−43] Those results point to the importance of the nitrile group in the chemisorption of ACN with transition metal

(38) (a) Horn, K.; Bradshaw, A. M.; Jacobi, K. *J. Vac. Sci. Technol.* **1978**, *15*, 575. (b) Widmark, P.-O.; Roos, B. O.; Siegbahn, P. E. M. *J. Phys. Chem.* **1985**, *89*, 2180. (c) Zaera, F.; Hall, R. B. *Surf. Sci.* **1987**, *180*, 1. (d) Zaera, F.; Fischer, D. A.; Carr, R. G.; Gland, J. L. *J. Chem. Phys.* **1988**, *89*, 5335.

(39) Matos, M.; Kirtman, B. *Surf. Sci.* **1995**, *341*, 162.

(40) (a) Bagotskaya, I. A.; Damaskin, B. B.; Kazarinov, V. E. *Russ. J. Electrochem.* **1994**, *30*, 263. (b) Panzram, E.; Baumgartel, H.; Roelfs, B.; Schroter, C.; Solomun, T. *Ber. Bunsen-Ges. Phys. Chem.* **1995**, *99*, 827. (c) Villegas, I.; Weaver, M. J. *J. Am. Chem. Soc.* **1996**, *118*, 458. (d) Morin, S.; Conway, B. E.; Edens, G. J.; Weaver, M. J. *J. Electroanal. Chem.* **1997**, *421*, 213. (e) Roefls, B.; Schröter, C.; Solomun, T. *Ber. Bunsen-Ges. Phys. Chem.* **1997**, *101*, 1105.

(41) (a) Hemminger, J. C.; Muetterties, E. L.; Somorjai, G. A. *J. Am. Chem. Soc.* **1979**, *101*, 62. (b) Kishi, K.; Ikeda, S. *Surf. Sci* **1981**, *107*, 405. (c) Friend, C. M.; Muetterties, E. L.; Gland, J. L. *J. Phys. Chem.* **1981**, *85*, 3256. (d) Wexler, R. M.; Muetterties, E. L. *J. Phys. Chem.* **1984**, *88*, 4037. (e) Hochard, F.; Jobic, H.; Clugnet, G.; Renouprez, A.; Tomkinson, J. *Catal. Lett.* **1993**, *21*, 381.

(42) Bigot, B.; Delbecq, F.; Peuch, V. H. *Langmuir* **1995**, *11*, 3828.

Table 4. Adsorption Geometries and Binding Energies (E_b) of ACN on $Ni_{16}(100)$

	Bond length (Å)				C1−C2−N angles (°)	E_b (kcal/mol)
	C1−C2	C2−N	C2−Ni	N−Ni		
ACN	1.440	1.166			180	
[ACN^1-$Ni_{16}(100)$]	1.431	1.171		1.75	179	−1
[ACN^2-$Ni_{16}(100)$]	1.493	1.300	1.90	1.97	123	−29
			1.99	1.76		
[ACN^3-$Ni_{16}(100)$]	1.494	1.332	1.96	1.85	123	−26
			1.93	1.78		

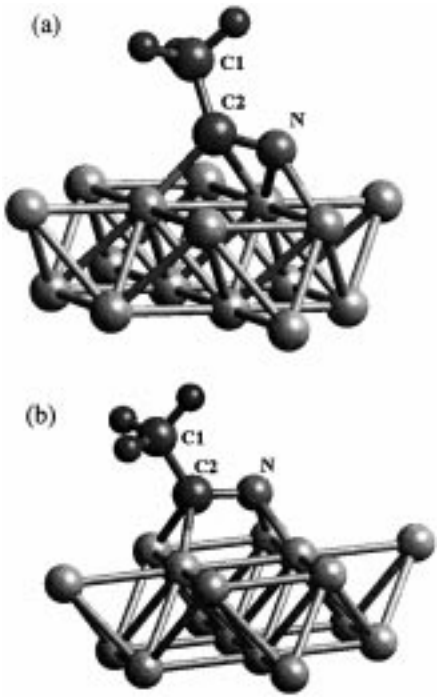

Figure 6. Sketch of the structure of ACN chemisorbed on the $Ni_{16}(100)$ surface: (a) [ACN^2−$Ni_{16}(100)$]; (b) [ACN^3−$Ni_{16}(100)$].

surfaces. Two bonding configurations are possible: ACN is either π-bonded by means of the nitrile group or bonded via the electronic lone pair of the nitrogen atom.

Three adsorption geometries of ACN are investigated on the $Ni_{16}(100)$ surface. The first adsorption geometry we consider consists of a perpendicular orientation of ACN, which interacts with the surface by means of the nitrogen atom. The electrons of the nitrogen lone pair overlap with the 3d, 4s atomic orbitals of one nickel atom. This adsorption geometry was first proposed for the copper surface.[44] The geometry of ACN adsorbed in that way on $Ni_{16}(100)$, a complex we refer to as [ACN^1−$Ni_{16}(100)$] (the numbering of the ACN^n−$Ni_{16}(100)$ complexes should not be confused with the various ethylene adsorption sites), is found to be only weakly distorted (bond lengths and bond angles are very close to their values in the isolated molecule, see Table 4) and the binding energy is very small (−1 kcal/mol). This observation agrees with the suggestion of Kishi and Ikeda[41b] that such an adsorption geometry occurs only at low temperature. The other two adsorption geometries, described in Figure 6, [ACN^2−$Ni_{16}(100)$] and [ACN^3−Ni_{16}-(100)], are found to be much more stable (−29 and −26 kcal/mol, respectively). In these two complexes, ACN interacts with the nickel cluster via both atoms of the nitrile group. To our knowledge, only one theoretical study, using an Extended Hückel method, has been performed on these systems;[42] it indicates that ACN adsorbed as in the [ACN^3- $Ni_{16}(100)$] complex provides the most-stable configuration on Ni(100). Note also that our results are in agreement with experimental studies that indicate the adsorption of ACN onto a polycrystalline Ni surface,[41b] on Raney nickel,[41e] or onto Ni(111)[41a,c] involves both atoms of the nitrile group, which are covalently bound to nickel atoms.

The geometry of the [ACN^2−$Ni_{16}(100)$] complex has the nitrile group positioned at ≅1.45 Å on top of the surface (Figure 6a). This orientation allows the formation of four covalent bonds (Table 4): two between C2 and the two central nickel atoms, and two between the nitrogen atom and two nickel atoms. Note that only three nickel atoms are involved, one of which interacts with both the carbon and nitrogen atoms. In the second complex, [ACN^3−$Ni_{16}(100)$], the nitrile group is quasi-parallel to the nickel cluster surface, above a four-Ni-square site (Figure 6b). This moiety interacts with the four-Ni site via four covalent bonds: two between C2 and two nickel atoms, and two between the nitrogen atom and the other two nickel atoms of the square site (Table 4). The global position of the nitrile group on the surface is not very different in [ACN^2−$Ni_{16}(100)$] and in [ACN^3−$Ni_{16}(100)$]; these two adsorption geometries likely correspond to two minima close to each other.

The [ACN^2−$Ni_{16}(100)$] and [ACN^3−$Ni_{16}(100)$] geometries show strong similarities: With respect to the isolated ACN molecule, the C1−C2 bond length increases by 0.05 Å, the C≡N triple bond elongates by >0.1 Å and the C1−C2−N bond angle decreases from 180° to 123°. All these features result from an increase in hybridization of the atoms of the nitrile group, since they form new bonds with the nickel atoms. These geometry changes after chemisorption can be related to vibrational frequency modifications. A vibrational study of ACN adsorbed on Ni(111)[41c] shows a strong decrease in the vibrational frequency of the C≡N stretching (from 2267 to 1700 cm^{-1}), which is consistent with an elongation of this bond. The presence of a new peak in the HREELS spectrum of adsorbed ACN has been suggested to originate either in a significant modification of the C1−C2−N bending (from 361 to 520 cm^{-1}) or from Ni−N stretching. A tensor LEED analysis[43] for ACN adsorbed onto Ni(111) reveals that: (i) the nitrile group is quasi-parallel to the nickel surface; (ii) the C≡N bond length is estimated to be 1.28 ± 0.15 Å; and (iii) the C1−C2−N angle is 123° ± 15°; all these data are in very good agreement with the calculated values for models [ACN^2−$Ni_{16}(100)$] and [ACN^3−$Ni_{16}(100)$] (Table 4).

From preliminary calculations on different crystal faces, we find that ACN chemisorption is similar on the Ni(111) and Ni-(100) surfaces and that the experiment/theory comparison presented above is meaningful. Chemisorption can also be characterized by partial charge transfer between metal surface and adsorbate. This charge transfer is due to a rearrangement of the charge distribution after the formation of chemical bonds at the metal/molecule interface. Atomic charge partitioning using Mulliken or Hirshfeld methods[45] indicates a partial charge

(43) Gardin, D. E.; Barbieri, A.; Batteas, J. D.; Vanhove, M. A.; Somorjai, G. A. *Surf. Sci.* **1994**, *304*, 316.
(44) Sexton, B. A.; Hughes, A. E. *Surf. Sci.* **1984**, *140*, 227.

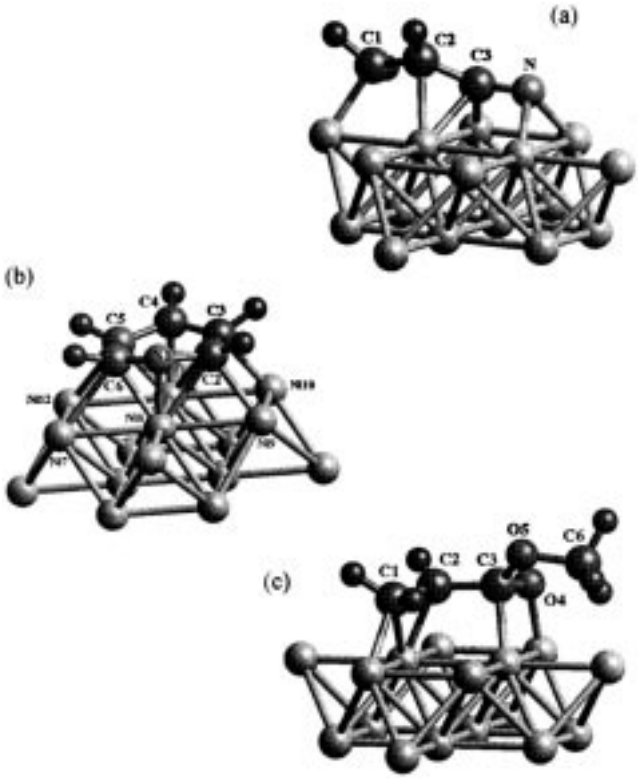

Figure 7. Sketch of the structure of (a) AN, (b) Py, and (c) MA chemisorbed on the $Ni_{16}(100)$ surface.

transfer from the metal cluster to ACN: electron density increases on C2 and N. This feature can be related to X-ray photoelectron spectroscopy experiments with ACN adsorbed onto the polycrystalline nickel surface.[41b] These measurements showed a decrease in binding energies for C1s (from 287.0 to 284.5 eV) and N1s (from 400.2 to 398.0 eV), attributable to chemisorption on the nickel surface, consistent with the charge redistribution calculated here. On the basis of these arguments, we are confident that the theoretical methods and model systems we use here are appropriate to our study.

4.2.2.2. Acrylonitrile on Ni(100). The interaction of AN with the nickel surface consists of chemisorption involving the nitrile group;[19c,41d] this result is not surprising, given what has been mentioned above. No information is available concerning the possible contribution of the C═C double bond to the chemisorption process of AN on the nickel surface. However, contains experimental indications point to the ability of the C═C double bond to interact with transition metal surfaces: AN is chemisorbed onto Ag,[19d] Cu,[19a] and Au electrodes[46] by means of both the C═C double bond and the nitrile group; on Pt(111), AN is chemisorbed flat.[19c]

The adsorption geometry of AN on $Ni_{16}(100)$ (Figure 7a) and the interatomic distances between atoms of AN and nickel atoms (Table 5) indicate that all four atoms of the molecular backbone interact by forming covalent bonds with five nickel atoms. The C1═C2 double bond interacts with two nickel atoms, while the nitrile group forms four covalent bonds with four nickel atoms. Note that the position of the nitrile group of AN on top of four-Ni-square site is the same as that found for the most-stable ACN adsorbate ($[ACN^3-Ni_{16}(100)]$, see Figure 6b). The theoretical adsorption geometry of AN on $Ni_{16}(100)$ is thus consistent with the experimental data that indicate a flat chemisorption of AN on a nickel surface with the involvement of the nitrile group; moreover, this theoretical model confirms that the C═C double bond is also involved in the interaction with the nickel surface.

Table 5. Geometric Structure of AN Adsorbed onto $Ni_{16}(100)$

	bond lengths (Å)	
bond	AN	AN-Ni_{16} (100)
C1−C2	1.336	1.450
C2−C3	1.410	1.433
C3−N	1.169	1.330
C1−Ni		1.90
C2−Ni		1.97
C3−Ni		1.94, 1.85
N−Ni		1.86, 1.82

The type of adsorption for $[AN-Ni_{16}(100)]$ can be characterized as a di-π-adsorption, in contrast to a di-σ-adsorption onto Cu(100).[14,16,19a] In the di-π-adsorption process occurring in $[AN-Ni_{16}(100)]$, all $2p_\pi$ atomic orbitals originally involved in the C1−C2 and C3−N bonds now interact with the 3d and 4s atomic orbitals of Ni. The C1−C2, C3−N, and C2−C3 bonds elongate by 0.12, 0.02, and 0.16 Å, respectively (Table 5). An important consequence of the modification in hybridization of the AN atoms is that the C1−H bonds tilt away from the plane of the double bond. Along the same line, the C2−C3−N group acquires an angle of 165° instead of 180° in the isolated molecule. The calculated binding energy of the $[AN-Ni_{16}(100)]$ complex is −43 kcal/mol.

4.2.2.3. PY on Ni(100). Molecular adsorption of PY, first studied on mercury electrodes, is nowadays intensively studied on transition metal surfaces under ultrahigh vacuum condition[47,48] or in contact with an electrochemical solution.[49] In aqueous solution, the molecular chemisorption of PY on metal electrodes is reversible[49a] and was described by means of a Frumkin isotherm.[49c] On transition metal surfaces, PY is either π-bonded flat on the surface, N-bonded perpendicular to the surface, or N/π-bonded flat or tilted. The orientation of PY mainly depends on the coverage and temperature.

Two models are considered here: In the first one, PY is put flat on the $Ni_{16}(100)$ surface (Figure 7b). In the second complex, PY is perpendicular to the surface, with the nitrogen atom pointing toward the surface. After geometry optimization and evaluation of the binding energy, we find the second complex less stable than the first one. Consequently, we focus only on $[PY-Ni_{16}(100)]$, where PY is adsorbed flat on the surface; its geometric features are given in Table 6 and the binding energy is −10 kcal/mol. The higher stability of flat-adsorbed PY is in agreement with experimental data showing that, at low surface coverage and low temperature, PY is adsorbed parallel to the Ni(100) surface[48a] as well as to the low-index surfaces Ni(111)[48b] and Ni(110).[48c] In the adsorption model shown in Figure 7b, adsorbed PY presents nearly Cs symmetry; HREELS experiments also indicate Cs symmetry for adsorbed PY on Ni(100).[48a] Another direct indication of the involvement of carbon and nitrogen atoms in the chemisorption of PY on nickel surfaces[48] is the decrease in both C1s and N1s core electron-binding energies due to chemisorption. This experimental observation is consistent with the $[PY-Ni_{16}(100)]$ complex showing an

(45) Hirshfeld, F. L. *Theor. Chim. Acta* **1977**, *44*, 129.
(46) (a) Bewick, A. *J. Electroanal. Chem.* **1983**, *150*, 481. (b) Gao, P.; Weaver, M. J. *J. Phys. Chem.* **1985**, *89*, 5040.
(47) Haq, S.; King, D. A. *J. Phys. Chem.* **1996**, *100*, 16957
(48) (a) DiNardo, N. J.; Avouris, P.; Demuth, J. E. *J. Chem. Phys.* **1984**, *81*, 2169. (b) Cohen, M. R.; Merrill, R. P. *Langmuir* **1990**, *6*, 1282. (c) Cohen, M. R.; Merrill, R. P. *Surf. Sci.* **1991**, *245*, 1. (d) Kishi, K.; Kikui, F.; Ikeda, S. *Surf. Sci.* **1980**, *99*, 405.
(49) (a) Lipkowski, J.; Stolberg, L.; Yang, D. F.; Pettinger, B.; Mirwald, S.; Henglein, F.; Kolb, D. M. *Electrochim. Acta* **1994**, *39*, 1045. (b) Brolo, A. G.; Irish, D. E.; Lipkowski, J. *J. Phys. Chem. B* **1997**, *101*, 3906; (c) Lust, E.; Jänes, A.; Lust, K. *J. Electroanal. Chem.* **1997**, *425*, 25.

Table 6. Geometric Structure of Pyridine (PY) Adsorbed Flat on $Ni_{16}(100)$

	bond lengths (Å)	
bond	PY	[PY-$Ni_{16}(100)$]
N1−C2	1.333	1.403
C2−C3	1.386	1.472
C3−C4	1.386	1.446
C4−C5	1.386	1.441
C5−C6	1.386	1.463
C6−N1	1.333	1.392
N1−Ni8	-	1.88
C2−Ni8	-	2.22
C2-Ni9	-	2.04
C3−Ni11	-	2.28
C3-Ni12	-	2.05
C4−Ni11	-	1.91
C5-Ni10	-	2.28
C5-Ni11	-	2.03
C6-Ni7	-	2.32
C6-Ni8	-	2.02

Table 7. Geometric Structure of Methyl Acrylate (MA) Adsorbed on $Ni_{16}(100)$

	MA	[MA-$Ni_{16}(100)$]
bond length (Å)		
C1−C2	1.331	1.453
C2−C3	1.461	1.475
C3−O4	1.222	1.330
C3−O5	1.346	1.385
O5−C6	1.425	1.421
C1−Ni7	-	2.02
C1−Ni8	-	2.07
C2−Ni8	-	1.94
C3−Ni9	-	1.87
O4−Ni10	-	1.85
O5−Ni9	-	2.68
bond angle (deg)		
C1−C2−C3−O5	0	−49.2

increase in partial Hirshfeld charge, (i.e., electronic density) on these atoms after complexation. All these aspects of agreement between theory and experiment favor the validity of the [PY−$Ni_{16}(100)$] complex as a model for the actual adsorbate.

In the complex, 10 interatomic distances between carbon or nitrogen atoms and nickel atoms are <2.35 Å (Table 7). All the backbone atoms of PY are covalently bonded to $Ni_{16}(100)$, because of significant overlap between the $2p_\pi$ atomic orbitals of carbon and nitrogen and the 3d and 4s levels of six nickel atoms (numbered 7 to 12 in Figure 7b). The shortest bond lengths are those involving the nitrogen atom (Ni8−N1 = 1.88 Å) and the carbon atom located para to N (Ni11−C4 = 1.91 Å). The backbone of PY is distorted from the chemisorption; the C═C and C═N bonds elongate by an average of 0.07 Å; the molecule becomes less planar, and the hydrogen atoms drift out of the plane of the molecule.

The replacement of chemisorbed organic species by other molecules in the gas phase gives an indication about the reversibility of the adsorption and the relative adsorbability of the molecules. PY is known to displace a chemisorbed layer of benzene on a polycrystalline nickel surface;[48d] in contrast, it is not able to displace a chemisorbed layer of ACN.[41b] Our calculations are consistent with these observations since ACN is found to be more strongly chemisorbed than PY, the respective binding energies being −29 and −10 kcal/mol.

4.2.2.4. Methyl acrylate on Ni(100). To our knowledge, the adsorption of MA onto transition metal surfaces has not been studied. Nevertheless, some studies indicate that the adsorption of acrylic acid on Pt(100) from a neutral solution occurs partially via the C═C double bond and to some extent via the anionic carboxylate group.[50] In our optimized model, MA is bound to the nickel cluster with a binding energy of −14 kcal/mol. The adsorbate interacts with $Ni_{16}(100)$ by means of both the C═C double bond and the C═O group (Figure 7c). The interatomic distances between the oxygen or the carbon atoms and the four nickel atoms involved range between 1.85 and 2.07 Å (Table 7). The C1═C2 and C3═O4 bonds undergo an elongation of 0.12 and 0.11 Å, respectively. The $2p_\pi$ atomic orbitals of the carbon (C1, C2, C3) and O4 oxygen atoms overlap with the 3d and 4s levels of four nickel atoms (Ni7, Ni8, Ni9, Ni10). The hybridization of the carbon and oxygen atoms increases toward a sp^3 character, which is reflected by changes in torsion angles. For instance, the C1−C2−C3−O5 torsion angle goes from 0° to −49.2° after chemisorption; as a result, the oxygen atom of the methoxy group remains relatively far from the closest nickel atom (O5−Ni9 = 2.68 Å), and the hydrogen atoms of the methyl group do not interact significantly with Ni.[9]

4.2.2.5. N,N-Dimethylformamide on Ni(100). For this molecule, no chemisorption is found at the GC-DFT level. We thus consider the binding energy of DMF on $Ni_{16}(100)$ to be close to zero. This is consistent with the fact that no experimental studies have shown chemisorption for DMF on nickel surfaces.

5. Discussion

5.1. Solvent/Monomer Competitive Adsorption. On one hand, the experimental observations have shown that the possibility of obtaining a grafted polymer film depends on the monomer/solvent pair, and that the prepeak observed on the voltammogram is related to an electrografting reaction. The solvent thus obviously constitutes an important factor in the electrografting mechanism. On the other hand, it has been pointed out that monomer adsorption is a necessary step to produce grafted polymer chains. Indeed, if there is no adsorption of the monomer on the metal electrode at electrochemical potentials less cathodic than the reduction potential of the monomer in solution, then the reduced anionic monomer is repelled from the vicinity of the negatively charged surface of the cathode; consequently, polymerization starts in solution and no grafted polymer film can be formed. The presence of the monomer adsorbed at the metal surface before cathodic polarization of the nickel electrode therefore appears to be a prerequisite for electrografting. The monomer adsorption on the electrode surface can be hindered by the adsorption of solvent molecules, which would explain the importance of the solvent in the electrografting process. As a matter of fact, solvent molecules can chemisorb on the nickel surface from gas phase or from solution, as demonstrated in the previous section.

The assumption of competitive adsorption between solvent and monomer is reinforced when comparing the experimental observations and the binding energies calculated for the complexes. A close examination of Table 8 indicates that when the calculated binding energy (E_b) of the monomer is larger than that of the solvent ($\Delta E_b < 0$), the experiment leads to a grafted polymer film (e.g., as for the AN/ACN couple). In contrast, when the solvent is calculated to be more strongly bonded than the monomer (e.g., $\Delta E_b > 0$ for EA/ACN), then no grafted polymer film is observed.

At this stage, we can propose a semiqualitative explanation of the solvent influence, based on a simple model of adsorption from solution. The adsorption of the monomer from solution

(50) Katekaru, J. Y.; Garwood, G. A.; Hershberger, J. J. F.; Hubbard, A. T. *Surf. Sci.* **1982**, *121*, 396.

Table 8. Comparison between Experimental Observations and Calculated Coverage θ of the Metal Surface by the Monomer by means of the Frumkin isotherm (eq 9) with the Temkin parameter $r = 15$

pairs	ΔE_b (kcal/mol)	coverage θ^a	observations
AN/ACN	−17	0.85	grafting
AN/PY	−33	0.99	grafting
AN/DMF	−43	0.99	grafting
EA/ACN	+12	≅ 0	no grafting
EA/PY	−4	0.15	grafting
EA/DMF	−15	0.76	grafting

[a] $C_{M(sol)} = 0.1$ M.

can be represented by the following thermodynamic equilibrium:[20,21]

$$M(sol) + n\ S(ads) \rightleftharpoons M(ads) + n\ S(sol) + \Delta G_{ads} \quad (1)$$

The adsorption of one monomer molecule from the solution (M(sol)) onto the metal surface is accompanied by the desorption of n adsorbed solvent molecules (S(ads)). This equilibrium is characterized by the variation of the free enthalpy of adsorption (ΔG_{ads}). The presence of the electrolyte salt is neglected and the metal surface is supposed to be at its potential of zero charge. The term n in eq 1, called size factor, is defined as the number of solvent molecules replaced by one monomer. From the work of Nikitas,[51] who proposed an experimental way to evaluate the size factor, Trasatti[22] pointed out the difference between the theoretical value of n, as calculated from the molar volume ratio, and the experimental value, as obtained by Nikitas's method. The size factor obtained by the latter method is always close to 1, even for molecules for which the calculated size factor can be as high as 8. To explain that observation, Nikitas suggested a model based on the existence of adsorbed solvent clusters.[23] On the basis of this argument and the fact that the solvent and monomer molecules studied here have rather similar sizes, we can safely consider that the size factor n is equal to 1. The dependence between the surface coverage θ (i.e., the fraction of the maximal surface concentration of monomer on the nickel surface) and the concentration of monomer in solution ($C_{M(sol)}$) and the ΔG_{ads} of reaction 1 can be formulated from the expression of the equilibrium of reaction 1 as follows:[24]

$$(C_{M(sol)}/C_{S(sol)}) \exp(-\Delta G_{ads}/RT) = \theta/(1 - \theta) \quad (2)$$

where $C_{S(sol)}$ is the concentration of the solvent. This adsorption isotherm is a Langmuir-type isotherm[24] that describes the competitive adsorption between monomer and solvent molecules. Note that in this approach, the free enthalpy of adsorption ΔG_{ads} does not depend on coverage; however, the behavior of adsorbed molecules in a number of electrochemical reactions is found to be consistent with the assumption of a linearly decreasing apparent standard Gibbs energy of adsorption with coverage θ:[24]

$$\Delta G_{ads}(\theta) = \Delta G^\circ_{ads} + r\theta \quad (3)$$

ΔG°_{ads} is the free adsorption enthalpy at low monomer coverage. This variation of the adsorption energy with the monomer surface coverage, characterized by the Temkin parameter r, is a way to take into account the intrinsic heterogeneity of the surface and the lateral interactions changes between adsorbed molecules (including the electrostatic repulsion between the partial charges, due to chemisorption, carried by the same adsorbed species). At low coverage, the more reactive species (solvent or solute) interacts with the reactive surface sites having the highest adsorption energy; at higher coverage, adsorption can only occur on the less-reactive surface sites. The injection of this coverage function $\Delta G_{ads}(\theta)$ into the Langmuir-type isotherm gives the Frumkin isotherm:[24]

$$(C_{M(sol)}/C_{S(sol)}) \exp(-\Delta G^\circ_{ads}/RT) = \theta/(1 - \theta)\exp(r\theta/RT) \quad (4)$$

The concentrations of the solvent and monomer in the electrochemical medium are linked through the following expression:

$$C_{S(sol)} = (d_{S(sol)}/F_S)\ [1000 - C_{M(sol)} \cdot (F_M/d_{M(sol)})] \quad (5)$$

where $d_{S(sol)}$ and $d_{M(sol)}$ are the densities of solvent and monomer, and F_S and F_M are their molar masses.

The variation of the free enthalpy of adsorption, ΔG°_{ads}, is the difference in free enthalpy of adsorption of the monomer ΔG_{Mads} and the solvent ΔG_{Sads}:

$$\begin{aligned}\Delta G^\circ_{ads} = \Delta G_{Mads} - \Delta G_{Sads} &= [\Delta H_{Mads} - T\Delta S_{Mads}] - [\Delta H_{Sads} - T\Delta S_{Sads}] \\ &= (\Delta H_{Mads} - \Delta H_{Sads}) - T(\Delta S_{Mads} - \Delta S_{Sads}) \\ &= \Delta H_{ads} - T\Delta S_{ads} \quad (6)\end{aligned}$$

where ΔH_{Mads} and ΔH_{Sads} are the enthalpic variations accompanying the adsorption of the monomer and the solvent from solution, respectively, and ΔS_{Mads} and ΔS_{Sads} are the entropic variations after the adsorption of the monomer and the solvent from solution. The adsorption of a molecule from solution involves a partial desolvation (the removal of about half of the solvation sphere surrounding the molecule in solution), followed by its adsorption on the metal surface, the replacement of another species, that is, the desorption of a previously adsorbed species and the partial solvation of the desorbed molecule. The total entropic variation ($\Delta S_{Mads} - \Delta S_{Sads}$) following the adsorption of the monomer is expected to play an increasing role as the size difference between the components increases[29a] and as the adsorption modifies the local order in the liquid (which is not negligible when specific intermolecular interactions, e.g., hydrogen bonds, exist). Here, since the sizes of the monomer and the solvent molecules are comparable and there is no specific interaction between solvent and monomer molecules, the total entropic variation should be small; it is thus reasonable to neglect the entropic terms.

The adsorption enthalpy of the solvent (ΔH_{Sads}) or monomer (ΔH_{Mads}) from solution is equal to the difference between the partial desolvation energy and the adsorption energy of the molecule with the metal surface. The energy needed for the partial desolvation can be approximated as one half of the enthalpy of vaporization (ΔH_{vap}) from its pure liquid phase since there are no specific intermolecular interactions in the solvent/monomer solution. The adsorption energy of the molecule with the metal-surface phase can be approximated as the calculated binding energy. Because of solvation effects, the adsorption energy of a molecule from the gas phase is always higher than that from solution. Note that the solvents and monomers used here should have similar enthalpies of vaporization since, at 298 K, $^1/_2\Delta H_{vap}$[52] is 3.94 kcal/mol for ACN, 4.31 kcal/mol for CH_3CH_2CN (similar to AN), 4.69 kcal/mol for CH_3CH_2-$COOCH_2CH_3$ (similar to EA), 4.81 kcal/mol for PY, and 5.61

(51) Nikitas, P. *J. Electroanal. Chem.* **1988**, *263*, 147.

(52) Lide, D. R. *Handbook of Chemistry and Physics*, 76th ed; CRC Press: New York, 1995.

kcal/mol for DMF. Hence the binding energy for both the monomer and the solvent, can reasonably be decreased by 5 kcal/mol to better estimate the adsorption energy of the molecule from solution. For the polar molecules we consider, we expect no dramatic differences in lateral interaction energy for the following pairs: solvent/solvent, solvent/monomer, and monomer/monomer. On this basis, when the adsorbate replaces the solvent at the interface, the energy variation from these lateral interactions is negligibly small (this is different from the modification of the lateral interactions when the coverage is increased).

As far as competitive adsorption is concerned, since (i) the partial desolvation energy is the same for the solvent and the monomer, (ii) the lateral interaction can be neglected, and (iii) the order of reactivity of the various molecules interacting with $Ni_{16}(100)$ is expected to be the same as on the actual Ni(100) surface, then the difference in binding energy, $E_{b[M-Ni_{16}(100)]} - E_{b[S-Ni_{16}(100)]}$, can be used to evaluate qualitatively the variation in enthalpy of adsorption ΔH_{ads} from solution. Note that we considered only one adsorption site represented by the Ni_{16}-(100) cluster, as this model provides reliable adsorption geometries for the adsorbates. In the isotherm, the lateral interaction modification with coverage and the heterogeneity of the surface can be explicitly taken into account by considering a nonzero value for the Temkin parameter r (eq 4). Using these approximations, we can directly relate the enthalpic variation ($\Delta H_{Mads} - \Delta H_{Sads}$) to the binding energy difference of the complexes [M−Ni_{16}(100)] and [S−Ni_{16}(100)]:

$$\Delta H_{ads} = \Delta H_{Mads} - \Delta H_{Sads} = E_{b[M-Ni_{16}(100)]} - E_{b[S-Ni_{16}(100)]} \quad (7)$$

Since we can neglect the entropic modification for adsorption from solution, the difference in binding energy [$E_{b[M-Ni_{16}(100)]} - E_{b[S-Ni_{16}(100)]}$] is used to approximate ΔG_{ads} of reaction 1:

$$\Delta G^{\circ}_{ads} \cong E_{b[M-Ni_{16}(100)]} - E_{b[S-Ni_{16}(100)]} \quad (8)$$

With these approximations, the following isotherm can be proposed:

$$(C_{M(sol)}/C_{S(sol)}) \exp[(E_{b[S-Ni_{16}(100)]} - E_{b[M-Ni_{16}(100)]})/RT] = \theta/(1-\theta) \exp(r\theta/RT) \quad (9)$$

In Table 8, the monomer coverage θ is calculated by considering a monomer concentration of 0.1 M and introducing the calculated binding energies $E_{b[M-Ni_{16}(100)]}$ and $E_{b[S-Ni_{16}(100)]}$ for isotherm 9 at $T = 300$ K, with a Temkin parameter $r = 15$. The exact value of this parameter is unknown in our case; the value $r = 15$ was chosen because it provides a reasonable isotherm with respect to those of naphthalene adsorbed on platinum electrode in aqueous basic solutions.[53] The influence of using the Temkin parameter, modeling the lateral interactions and the heterogeneity of the metal surface, is displayed in Figure 8a. For $r = 0$, the Frumkin isotherm corresponds to the Langmuir isotherm, which is well-known to overestimate the coverage by neglecting lateral interactions and surface heterogeneity. By considering positive values of r, which is related to the repulsion of the adsorbed molecules when coverage increases, the evolution of the coverage becomes smoother than in the Langmuir isotherm. Despite the qualitative aspect of the description of the phenomenon, we find a remarkable agreement

(53) Bockris, J. O. M.; Green, M.; Swinkels, D. A. J. *J. Electrochem. Soc.* **1964**, *111*, 743.

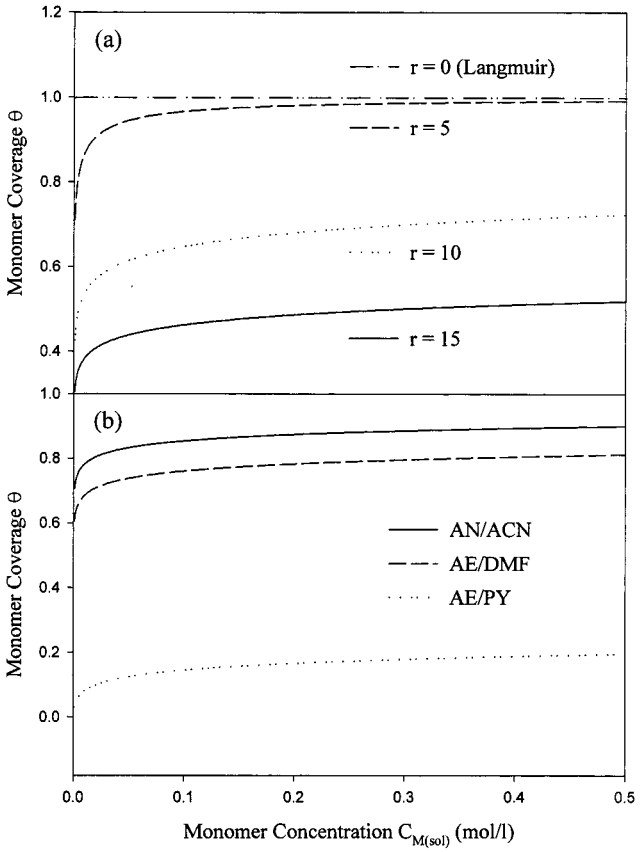

Figure 8. (a) Influence of the Temkin parameter, r, on the shape of the Frumkin adsorption isotherm for a model monomer/solvent pair ($F_M = F_S = 50$, $d_M = d_S = 1$, $T = 300$ K, $\Delta G_{ads} = -10$ kcal/mol); (b) Frumkin isotherm ($T = 300$ K) for different solvent/monomer pairs: AN/ACN, AE/PY, AE/DMF.

between the calculated coverage θ and the experimental observations (Table 8, Figure 8b):

For the AN monomer, $\theta > 0.85$ for all solvents. This suggests that when the nickel electrode is introduced in the electrochemical solution (whatever the solvent) and when the equilibrium of eq 1 is reached, the nickel surface is almost completely covered by a monolayer of AN molecules. Since the exponential factor, $\exp[(E_{b[S-Ni_{16}(100)]} - E_{b[M-Ni_{16}(100)]})/RT]$, is very large, the concentration of the monomer has little influence on the coverage. This effect is due to the strong chemisorption of AN and to the exponential factor, which further magnifies the difference in binding energy.

The situation is different with the EA monomer since it is less strongly bonded to nickel. Three different behaviors appear:

(i) For the ACN/EA pair, the solvent totally covers the nickel surface, the coverage related to the monomer being negligible. When the cathodic polarization is increased above the reduction potential of the monomer, the monomer molecules in solution are reduced. Consequently, polymerization is initiated and propagates in solution. Experimentally, no grafting is observed.

(ii) When DMF is used as solvent (Figure 8b), the EA monomer covers a large portion of the metal electrode ($\theta = 0.76$). The condition for obtaining a grafted chain is thus fulfilled and accordingly the formation of a grafted PEA film is observed.

(iii) Between these two cases, another situation occurs for the EA/PY couple. Since the binding energies of EA and PY are very close, the exponential term is rather small and the concentration term becomes important. Indeed, Figure 8b shows that for small monomer concentrations ($<10^{-2}$ M), the coverage

of the electrode by the monomer is very small at 300 K. Note that the surface concentration of monomer, which is proportional to the coverage, is a crucial factor in determining the density of grafted polymer chains at the metal electrode; this in turn influences the adherence of the polymer film. For the other pairs leading to grafted polymer films, the influence of the monomer concentration is less notable because the exponential term is large. Hence, concentration effects are significant only when ΔG_{ads} is small. Figure 8b shows that concentration plays an important role in the coverage of the electrode surface only for small ΔG_{ads}. For a small EA concentration in PY (e.g., $C_{M(sol)} = 10^{-3}$ M), the coverage is small ($\theta = 0.02$) and no grafting is experimentally observed, whereas for a higher concentration (e.g., $C_{M(sol)} = 0.5$ M), the coverage is increased ($\theta = 0.20$) and a grafted polymer film is obtained.

In conclusion, since the adsorption step of the monomer constitutes a crucial stage, it is possible to fulfill this grafting condition by adequately choosing the solvent. The solvent must be such that ΔG_{ads} is negative. For small ΔG_{ads}, two factors can significantly increase the coverage: a decrease in temperature, and an increase in monomer concentration. The coverage should also affect the adherence of the grafted polymer film, because the higher the monomer coverage, the higher the number of adsorbed reactive intermediates and the higher the density of grafted polymer chains.

5.2. Grafting Mechanism. Finally, our theoretical results suggest that the presence of the prepeak is related to the fact that the monomer adsorption is the first step of the electrografting mechanism. For a monomer strongly adsorbed onto the metal surface (e.g., AN in the various solvents used here), we have shown that the metal surface is mainly covered by the monomer.

The calculations indicate that, on adsorption, the lowest unoccupied molecular orbital (LUMO) of the monomer is split into several unoccupied levels, which are significantly stabilized with respect to the LUMO of the nonchemisorbed monomer. When cathodic polarization is applied, the energy of the electrons in the metal increases; electron transfer becomes possible at the metal/solution interface when the energy of the electrons in the metal reaches the energy of an acceptor electronic level.[54] This condition is first encountered for chemisorbed AN since unoccupied levels localized on AN are more stable relative to the LUMO of AN in solution; if the polarization is further increased, electron transfer to AN in solution can take place. Hence, the effect of chemisorption of AN on a metal surface is to provide electronic levels that are localized on AN and close to the Fermi level. In the voltammetry curve (Figure 2a), the prepeak current density could thus be associated with the reduction of the chemisorbed monomers, this reduction leading to the formation of AN radical-anions that remain chemisorbed on the surface. The stable adsorption of this product of reduction is supported by previous theoretical studies,[7c,16] which show that AN radical-anions remain chemisorbed on Ni(100) and Cu(100) surfaces, despite the electrostatic repulsion between the negative charge of AN and the electric field present in the vicinity of the cathode. These species thus model stable adsorbed reactive intermediates, similar to those proposed by Lécayon et al.,[2] which are likely to react with AN monomers coming from solution and then start the AN polymerization, thus leading to a grafted PAN chain. The decrease in current density of the prepeak could thus be related to the consumption of all the adsorbed AN molecules, thus giving the adsorbed reactive intermediates. These adsorbed reactive intermediates are then expected to react with the monomer molecules located in solution near the surface of the cathode. At this stage, diffusion is needed to carry new monomer molecules near the surface. The whole process can be summarized as follows for a strongly adsorbing monomer such as AN:

$$AN_{sol} + solvent_{ads} \rightleftharpoons AN_{ads} + solvent_{sol}$$

(monomer adsorption)

$$AN_{ads} + e^- \rightarrow (AN_{ads})^{-\cdot}$$

(electrochemical generation of a reactive intermediate)

$$(AN_{ads})^{-\cdot} + AN_{sol} \rightarrow (AN_{ads}\text{-}AN^{-\cdot})$$

(polymerization of a grafted chain)

6. Conclusions

We have reported on a joint experimental and theoretical study of the interaction of monomer or solvent molecules with Ni surfaces. Complexes modeling the interaction of an organic adsorbate with a transition metal surface, as described in the framework of the LSD approximation of the DFT, appear appropriate for studying the structure of the adsorbate/metal interface. The adsorption geometries and electronic density modifications found during chemisorption are consistent with a large number of experimental data. These complexes provide the first theoretical molecular models describing the adsorption on nickel of organic molecules as big as AN, EA, PY, or DMF; the C═O, C≡N, and C═C groups of the organic molecules are found to be involved in chemisorption of the organic sorbates on the nickel surface by means of chemical π-d interactions.

By considering the difference in binding energies (at the GC level of DFT) between the solvent and the monomer with the nickel cluster as a valid estimate of ΔG_{ads} in a Frumkin-type isotherm, a semiquantitative description of the electrografting phenomenon is reached. This description, which is in good agreement with the experimental observations, indicates that the first stage of the electrografting mechanism is the monomer adsorption, which can enter into a competitive adsorption with the solvent, when no cathodic polarization is applied. The chemisorbed monomer is seen as the species that is reduced during the prepeak observed in the voltammograms. This first reduction process gives rise to an adsorbed reactive intermediate that carries a negative charge and is able to react with a monomer in solution, which initiates the growth of a grafted polymer chain.

Very interestingly, this study opens the possibility of using the electropolymerization method to chemically graft a wider range of polymers onto transition metal surfaces. A basic means of the control is the appropriate choice of solvent.

Acknowledgment. This work is partly supported by the Belgian Federal Government "Service des Affaires Scientifiques, Techniques et Culturelle (SSTC)" in the framework of the "Pôle d'Attraction Interuniversitaire en Chimie Supramoléculaire et Catalyze Supramoléculaire (PAI 4/11)." The work in Mons is also supported by FNRS-FRFC and an IBM Academic Joint Study. X.C. is a grant holder of "Fonds pour la Formation à la Recherche dans l'Industrie et dans l'Agriculture (FRIA)." R.L. is "Maître de Recherches du Fonds National de la Recherche Scientifique (FNRS)."

JA981730Y

(54) Bockris, J. O. M.; Khan, S. U. M. *Quantum Electrochemistry*; Plenum Press: New York, 1979; chapt. 3.